Multi-frequency Large-Scale Channel Modeling and Green Networking Design

Zhenfeng Zhang(✉), Daosen Zhai, Ruonan Zhang, and Jiaxin Wang

Department of Communication Engineering, Northwestern Polytechnical University, Xi'an 710072, Shaanxi, China
2450182446@mail.nwpu.edu.cn

Abstract. In this paper, we conduct the measurement campaign in the urban microcell (UMi) outdoor-to-indoor (O2I) scenario, with the object to investigate the large-scale fading at 900 MHz, 2.6 GHz, and 3.5 GHz. Specifically, the path loss model is constructed based on the experimental data and the 3GPP TR36.873 channel model standard. Furthermore, according to the channel model, we propose a triple-band frequency-switching (TB-FS) scheme, which can minimize the transmitting power of a base station. Simulation results indicate that considering the propagation characteristics, the low frequency is preferred under small rate requirement and the high frequency is preferred under the large rate requirement. Furthermore, we find that the optimal spectrum is independent from positions of the devices. These results are valuable for the design and optimization of green communications and network deployment.

Keywords: Outdoor-to-indoor (O2I) · Channel measurement and modeling · Green communication

1 Introduction

In recent years, the mobile communications have made great progress all over the world. Meanwhile, the communication scenes also become more and more complicated. The fifth generation (5G) network will be available by 2020. There will be massive devices served by the 5G network, which leads to huge energy consumption. Therefore, the energy consumption should be taken into account in the 5G network design. The literature [1] proposed the concept of green communications. In order to improve the energy efficiency, it summarized five technologies including the device-to-device (D2D) communications, ultra dense networks (UDN), massive MIMO, spectrum sharing, and Internet of things (IoT).

This work was supported in part by the National Natural Science Foundation of China (61571370, 61601365, and 61801388), in part by the Fundamental Research Funds for the Central Universities (3102017OQD091 and 3102017GX08003), and in part by the China Postdoctoral Science Foundation (BX20180262).

B. Li et al. (Eds.): IoTaaS 2018, LNICST 271, pp. 367–375, 2019.
https://doi.org/10.1007/978-3-030-14657-3_37

In [2–6], the authors proposed the solutions from different aspects to reduce the communication energy consumption.

In various network deployment environments, the channel features are considerably different, which has a great influence on the wireless network design, such as the power allocation, relay deployment, spectrum utilization, and so on. Channel measurement in different bands can provide useful guidance for the green networking design. Motivated by these factors, abundant channel measurement activities have been conducted. For example, the measurement campaign in [7] investigated the Outdoor-to-Indoor (O2I) path loss in the metropolitan small cell scenario at 3.5 GHz. Based on the two-dimensional (2-D) O2I models given in M.2135 and Winner II, the authors modified the 2-D path loss model by adding a height gain. In [8], the 2.6 GHz O2I wireless link was measured in three metro environments (tunnel, station, and open field). The measurement results indicated that the attenuation in the metro environments were 15 to 20 dB higher than those in free space. It was obtained that the O2I channel followed a Rayleigh distribution and the impact of the window glasses on the signal attenuation was not significant for the overall link budget. The literature [9] characterized the 3-D spatial channels in a gymnasium by field measurement and statistical modeling. It was demonstrated that the average angular spreads were independent from the distance and direction of the microcell base station (BS) in the typical stand coverage scenario.

This article focuses on the outdoor-to-indoor (O2I) channel measurement and modeling at 900 MHz, 2.6 GHz, and 3.5 GHz. The contributions of this paper are two-fold. First, we conducted the urban microcell (UMi) O2I large-scale channel measurement in a hotel. The wireless links from the ground to the high building, where the BS was placed on the ground and the user equipment (UE) distributed on different floors, were measured. This measurement setup is termed as "low-to-high (L2H)" propagation. We then utilized the measurement data to modify the O2I channel model in the 3GPP TR38.673 standard [10]. The O2I path loss model can be used to calculate the transmitting power of the BS. Second, through the analysis of propagation characteristics at the three frequencies, we can obtain that combining hybrid frequencies for network coverage has much greater advantages in energy saving and high-capacity transmission than using a single frequency. We propose a triple-band frequency-switching (TB-FS) scheme, which can minimize the transmitting power of the BS under different rate requirements.

The remainder of this paper is organized as follows. Section 2 describes measurement system setup, and channel measurements. Section 3 describes measurement results. In Sect. 4, the O2I channel model in the 3GPP TR38.673 standard was modified using the measurement data. Section 5 presents triple-Band frequency-switching (TB-FS) scheme. Finally, conclusions are drawn in Sect. 6.

2 Measurement System

The measurement campaign was conducted in a hotel in Chengdu, China, and the environment was a typical UMi O2I scenario. The channel was measured

by a tri-band continuous-wave (CW) large-scale channel sounder as shown in Fig. 1. The transmitter (TX) emulated a base station of 2.5 m height placed on the ground, 30 m away from building, as shown in Fig. 1(a). The receiver (RX) was located on different floors, and its height was 1.5 m, as shown in Fig. 1(b). The RX was placed on five different floors, i.e., the 3rd, 4th, 6th, 8th, and 10th floors.

(a) Transmitter (b) Receiver

Fig. 1. Channel sounder for O2I scenario measurement.

On the TX side, the system is equipped with three RF chains at 900 MHz, 2.6 GHz and 3.5 GHz, and each of them consists of a signal generator, power amplifier (PA), and transmitting antenna. Based on the narrow-band sounding scheme, the TX system generates and transmits a single tone at each target carrier frequency. The RX system adopts a wideband antenna to receive the probing signals at all the three frequencies. The wideband antenna is omni-directional in the azimuth plane and has a half power beamwidth (HPBW) of 40° in the elevation dimension, with the maximum gain of 2.5 dBi. The received single-tone sounding signal is amplified by a low noise amplifier (LNA) and then input into a portable spectrum analyzer (SA). The SA is programmed to measure the received power at the marked frequency points continuously. In this system, we set three markers at the three frequencies. The SA measures the power at the first frequency for 50 times periodically with the interval of 300 ms, and then sends the data to a laptop via Ethernet for storage. Then, the process is repeated for the second and third frequencies.

The system needs to be calibrated before each test, because the transmitting power and gains of the RF equipments such as the amplifiers, change with temperature and time. Then, a path loss value of the specific channel can be obtained by calibrating the measured power attenuation. In what follows, we introduce the detailed calibration and field measurement processes. Firstly, the TX and RX systems are connected directly by radio cables, and an attenuator with −40 dB gain is inserted in the link in calibration, as shown in Fig. 2(a). In field measurements, the RF link is replaced by the transmitting and receiving antennas

and a wireless channel, as shown in Fig. 2(b). By comparing the received power with the calibration results, the attenuation over the radio channel is obtained.

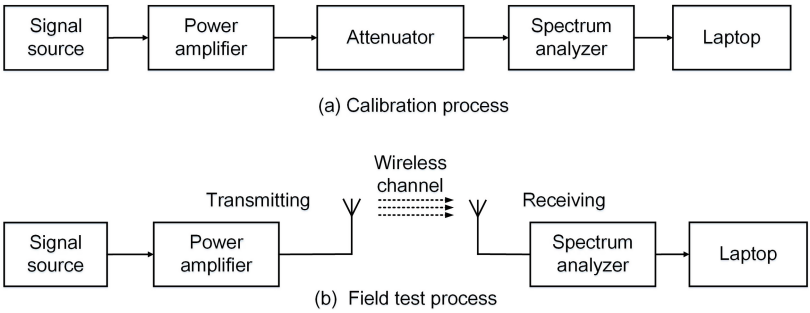

Fig. 2. Calibration and field test processes.

The path loss is calculated according to calibration and measurement procedures by

$$P_{TX} + G_{PA} + G_A - L = P_{RX1}, \tag{1}$$

$$P_{TX} + G_{PA} + G_{TX} - PL + G_{RX} - L = P_{RX2}, \tag{2}$$

where P_{TX} is the transmitting power which can be set manually, $G_{PA} = 10$ dB is the gain of the power amplifier and $G_A = -40$ dB is the attenuation of the attenuator. The gains of the transmitting and the receiving antennas are denoted by G_{TX} and G_{RX}, respectively. The radiation patterns of the antennas have been measured in an anechoic chamber. P_{RX1} and P_{RX2} are the received power in calibration and measurement, respectively, which are captured by the spectrum analyzer. L represents other losses in the measurement system such as the high-frequency phase-steady cable loss. According to (1) and (2), we can get path loss value PL by calibration.

3 Measurement Results

The contour diagram in Fig. 3 demonstrates the distributions of the path loss magnitude at the three frequencies of 900 MHz, 2.6 GHz, and 3.5 GHz. It is concluded that the penetration capability of the low frequency is better than that of the high frequency. We analyze the signal attenuation in the room and corridor as follows.

The rooms on the 3rd floor are representative, so we choose the 3rd floor as an example to analyze the path loss in the measurement scene. The path loss of Room 316 is significantly smaller than that of Room 315. Similarly, the path loss of Room 320 is significantly smaller than that of Room 319. This is because Rooms 316 and 320 are closer than to the TX, and the signal only needs to penetrate one wall to reach the rooms in this O2I scenario. In Room 315, the

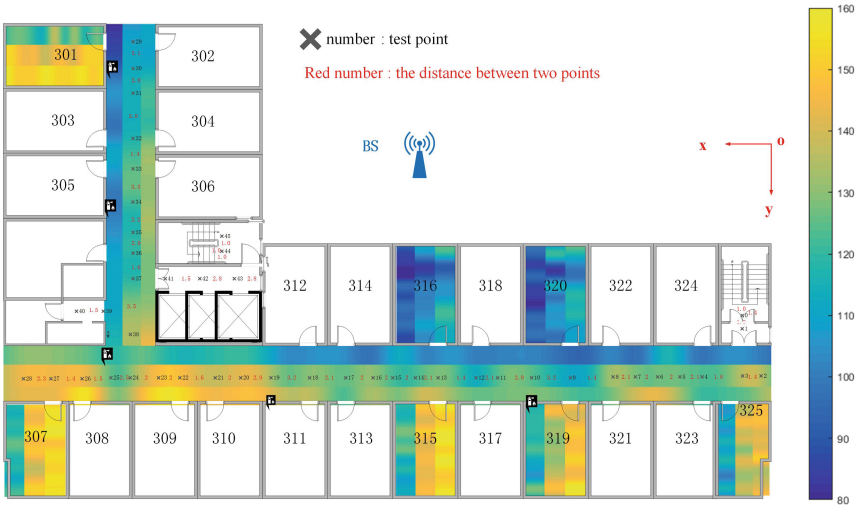

Fig. 3. Path loss on the 3rd floor at 900 MHz, 2.6 GHz, and 3.5 GHz.

signal needs to pass through three walls which causes great fading on the signal. Room 319 is similar to Room 315.

In the long corridor, the path loss at all the three frequencies is obviously larger than that in Rooms 316 and 320. This is because the signal penetrates double walls of the rooms to reach the corridor. We can see that the path loss in the middle of the long corridor is the smallest due to its shortest distance to the TX. From the middle to the right end, the path loss increases gradually with the increment of the distance between the TX to RX. However, the signal can enter the corridor at the right end by the reflection of other buildings outside. Thereby its path loss becomes small again. From the center to the left end, the path loss value increases significantly not only because of the increment of the distance to the TX, but also because the signals need to pass through the double rooms (or an elevator).

Similarly, at the top of the corridor vertical in Fig. 3, the signals have two paths to arrive at the RX. One path is the reflection by other surrounding buildings, and the other path goes through the two walls of Room 302. Thus the path loss is the smallest along the corridor. In the middle part, the path loss becomes low again due to the reduced distance to the TX. From the middle to the bottom part of the corridor, the path loss continuously increases due to the increment of the transmission distance and the obstruction of the rooms.

4 O2I Channel Model

According to the 3GPP TR38.673 channel standard, the O2I path loss of the UMi scenario can be expressed as

$$PL = PL_b + PL_{tw} + PL_{in}, \tag{3}$$

where PL_b, PL_{tw}, and PL_{in} are the outdoor path loss, wall penetration loss, and indoor path loss, respectively. In detail, PL_b, PL_{tw}, and PL_{in} are given by

$$\begin{cases} PL_b = PL_{3D\_UMi}(d_{3d\_in} + d_{3d\_out}), \\ PL_{tw} = 20, \\ PL_{in} = 0.5 d_{2d\_in}, \end{cases} \tag{4}$$

where PL_{3D_UMi} is the path loss in the UMi scenario, which can be estimated according to the measurement data in our measurement campaign. The specific expression is given as

$$PL_{3D\_UMi} = 22.0 \log_{10}(d_{3D}) + 28 + 20 \log_{10}(f_c), \tag{5}$$

where $d_{3D} = d_{3d\_in} + d_{3d\_out}$ denotes the spatial three-dimensional (3D) distance between the BS and UE. d_{2d_in} is the two-dimensional distance from the indoor receiving terminal to the external wall. The O2I model schematic is shown in Fig. 4.

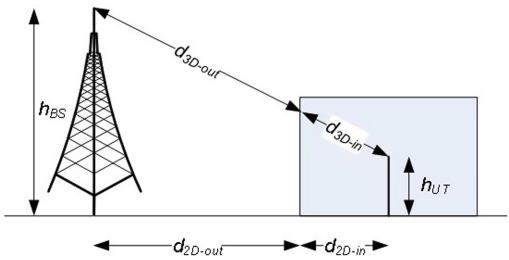

Fig. 4. The schematic of the O2I model [10].

When calculating the path loss with the O2I model, we need to determine the 3D distance between the TX and the RX. To achieve this goal, we need to establish a 3D coordinate system, as shown in Fig. 3. The right of the building is the y axis, and the horizontal position of the receiver is the x axis. The floor height is the z axis. By this way, the 3D coordinates of the BS and the measurement points are defined, and the 3D distance can be obtained. According to the triangular relationship, the 2D distance between the outer wall and the RX can be calculated.

Substituting the 2D and 3D distances and the three carrier frequencies into the O2I model given in (3) to (5), we can obtain PL_b and PL_{in}. Since the signals in the corridor needs to pass through two walls, the penetration loss PL_{tw} is larger than 20 dB given by the O2I model. This part is calculated by subtracting PL_b and PL_{in} from the real measurement data, and then we calculate the average to obtain the penetration loss of the two walls. Finally, the O2I path loss in the measurement scene can be obtained by adding the three parts, PL_b, PL_{in}, and PL_{tw}.

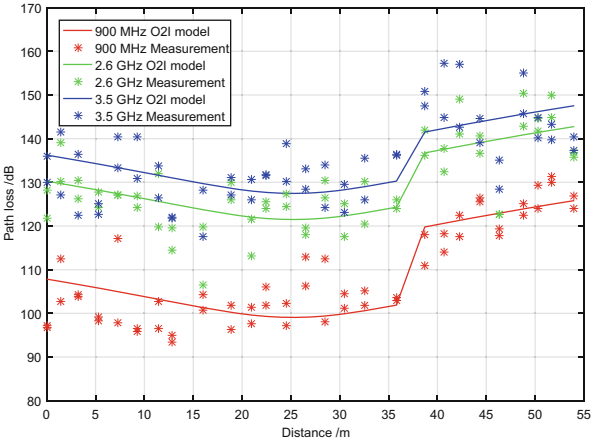

Fig. 5. Measurement results and O2I models.

The measured data and modified channel model are plotted in Fig. 5. As can be seen, the channel model fits the empirical results very well. The path loss when the distance is larger than 39 m becomes larger because the signals need to travel through two rooms or elevator.

5 Triple-Band Frequency-Switching (TB-FS) Scheme

To investigate the energy-saving spectrum allocation scheme, we calculate the transmitting power given data rate requirements according to the proposed channel model in Sect. 4 and the Shannon theorem. The specific parameter settings are as follows. The bandwidth of the 900 MHz carrier frequency is set as 180 KHz. Then according to the relationship of the carrier frequencies, the bandwidths at 2.6 and 3.5 GHz are set as 520 and 700 KHz, respectively. Thus the data rate and transmitting power can be

$$r_i = B_i log_2 \left(1 + \frac{P_i g_i}{n_0 B_i}\right), \tag{6}$$

$$P_i = \left(2^{\frac{r_i}{B_i}} - 1\right) \frac{n_0 B_i}{g_i}, \tag{7}$$

where r_i refers to the information transmission rate of the i-th carrier frequency, B_i denotes the bandwidth, P_i denotes the transmitting power, g_i denotes the channel power gain which can be obtained by the channel model, and n_0 refers to the noise power spectral density.

The numerical results are evaluated as follows. First, the rate r_i is set as a fixed value, and the transmitting power P_i at the three carrier frequencies is obtained according to the path loss model given in (3) and (7). Thus we take the transmission rate r_i as an independent variable to observe P_i in the band

of B_i. It can be observed from Fig. 6 that P_i at the three carry frequencies is different for the transmission rates. It can be seen that two of the three curves intercept with each other. This demonstrates that we can transmit signals at different frequencies and rates to minimize the transmitting power.

We analyze the relationship between the TX-RX distance and the rate intersecting point of the three lines. Interestingly, it is found that when the TX-RX distance is 50, 200 and 500 m, the rate intersecting point remains unchanged. This shows that the transmission rate is independent of the TX-RX distance. This observation indicates that the BS does not need to consider the location of the user when performing frequency switching at various data rates, which may significantly simplify the BS frequency switching operation. At the same time, it can be seen from the three sets of curves in Fig. 6 that if the BS utilizes the frequency switching technology, it can greatly reduce the power consumption.

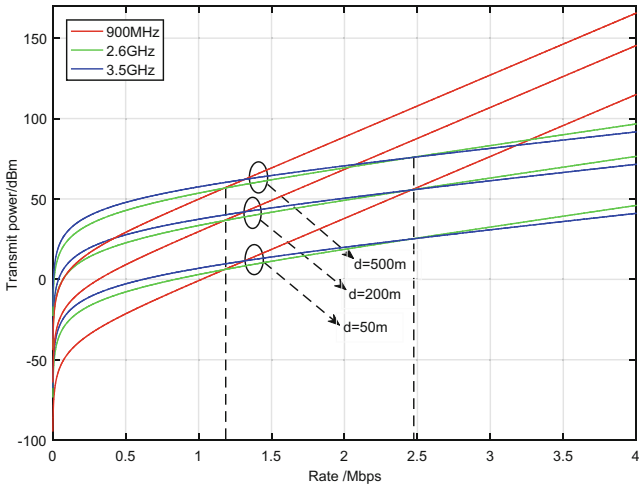

Fig. 6. The effect of the rate requirement on the transmission power.

6 Conclusion

In this work, we have performed a measurement campaign for the UMi O2I channels at 900 MHz, 2.6 GHz, and 3.5 GHz. We have constructed the O2I path loss model of the 3GPP TR36.873 standard based on our channel measurement results. The modified model indicates that the propagation loss through the concrete wall is very large. Furthermore, we have proposed the TB-FS scheme to save the BS power consumption. The numerical results show that the transmitting power at the three frequencies is independent from the TX-RX distance. As such, we can switch the carrier only according to the rate requirements to

reduce the BS transmitting power. The proposed channel model and TB-FS scheme can facilitate the development of green networks for the future mobile communication services.

References

1. Gandotra, P., Jha, R., Jain, S.: Green communication in next generation cellular networks: a survey. IEEE Access **5**(99), 11727–11758 (2017)
2. Lin, X., Andrews, J.G., Ghosh, A., Ratasuk, R.: An overview of 3GPP device-to-device proximity services. IEEE Commun. Mag. **52**(4), 40–48 (2014)
3. Chen, L., et al.: Green full-duplex self-backhaul and energy harvesting small cell networks with massive MIMO. IEEE J. Sel. Areas Commun. **34**(12), 3709–3724 (2016)
4. Goldsmith, A., Jafar, S.A., Maric, I., Srinivasa, S.: Breaking spectrum gridlock with cognitive radios: an information theoretic perspective. Proc. IEEE **97**(5), 894–914 (2009)
5. Kaushik, A., et al.: Spectrum sharing for 5G wireless systems (Spectrum sharing challenge). In: IEEE International Symposium on Dynamic Spectrum Access Networks (DySPAN), September 2015, pp. 1–2 (2015)
6. Gao, H., Ejaz, W., Jo, M.: Cooperative wireless energy harvesting and spectrum sharing in 5G networks. IEEE Access **4**, 3647–3658 (2016)
7. Li, C., Zhao, Z., Tian, L., Zhang, J.: Height gain modeling of outdoor-to-indoor path loss in metropolitan small cell based on measurements at 3.5 GHz. In: International Symposium on Wireless Personal Multimedia Communications (WPMC) (2014)
8. Arriola, A., et al.: Characterization of an outdoor-to-indoor wireless link in metro environments at 2.6 GHz. In: IEEE International Conference on ITS Telecommunications (2017)
9. Zhong, Z., Zhang, R., Ren, K., Wang, K., Li, B., Zhang, X.: Measurement and modeling of 3-dimensional radio channels with cross-polarizations in a gymnasium. In: IEEE European Conference on Antennas and Propagation, pp. 2473–2477 (2017)
10. 3GPP TR36.873-V12.4.0(2017–03) Study on 3D channel model for LTE